Inorg. Chem. **2007**, *46*, 2659–2665

Two-Photon Antenna Effect Induced in Octupolar Europium Complexes

Alexandre Picot,[†] Floriane Malvolti,[†] Boris Le Guennic,[†] Patrice L. Baldeck,[‡] J. A. Gareth Williams,[#] Chantal Andraud,*[,†] and Olivier Maury*[,†]

Laboratoire de Chimie, UMR CNRS-ENS-Lyon 5182, 46 Allée d'Italie, F-69364 Lyon Cedex 07, France, Laboratoire de Spectrométrie Physique, Université Joseph Fourier, BP 87 F-38402 Saint Martin d'Hères, France, and Department of Chemistry, University of Durham, South Road, Durham, DH1 3LE, U.K.

Received November 16, 2006

The synthesis of new chromophore-based pyridine-dicarboxamide ligands and related D_3 symmetric europium(III) complexes is described. The photophysical properties of the ligands and the complexes were thoroughly investigated and interpreted on the basis of theoretical calculations (TD-DFT). Finally, the luminescence of Eu(III) was sensitized by two-photon absorption of the ligand, illustrating the two-photon antenna effect phenomenon.

Introduction

Two-photon excitation (TPE) is an elegant way to promote a molecule to an excited electronic state, and its intrinsic confocal character, which arises from the requirement for a high photon flux, has triggered the emergence of high-resolution 3D resolved photochemistry. This new field of research has been greatly facilitated by the development of suitable femtosecond-pulsed laser sources and nonlinear microscopes. Promising applications have been described in the field of materials science for optical storage,[1] optical limitation,[2] and microfabrication,[3] as well as in biology for imaging,[4] drug delivery,[5] and photodynamic therapy.[6] This rapid development has prompted the scientific community to revisit "classical" photochemistry and has stimulated the design of new chromophores featuring optimized two-photon absorption cross-sections.[7]

Within this context, TPE antenna effects, defined as the TPE of an antenna chromophore followed by energy transfer to an acceptor moiety, become a challenging new frontier with exciting applications. For instance, the TPE of light-harvesting chromophores, followed by energy transfer to a porphyrin core, results in a significant enhancement in singlet oxygen production which is of prime importance for photodynamic therapy.[6b,8] On the other hand, FRET (fluorescence resonance energy transfer) has been successfully induced between TPE carotenoid and bacteriochlorophylls in studies of the photosynthetic process.[9] Finally, a two-photon antenna effect has been used to sensitize the luminescence of europium and terbium(III) directly linked to a protein.[10] These pioneering results open the way for the

* To whom correspondence should be addressed. E-mail: olivier.maury@ens-lyon.fr.
† Ecole Normale Supérieure de Lyon.
‡ Université Joseph Fourier.
# University of Durham.

(1) Cumpston, B. H.; Ananthavel, S. P.; Barlow, S.; Dyer, D. L.; Ehrlich, J. E.; Erskine, L. L.; Heikal, A. A.; Kuebler, S. M.; Sandy-Lee, I.-Y.; McCord-Maughon, D.; Qin, J.; Röckel, H.; Rumi, M.; Wu, X.-L.; Marder, S. R.; Perry, J. R. *Nature* **1999**, *398*, 51−54.
(2) (a) Wang, S.; Gang, Q.; Zhang, Y.; Li, S.; Xu, H.; Yang, G. *Chem. Phys. Chem.* **2006**, *7*, 935−941. (b) Dini, D.; Calvete, M. J. F.; Hanack, M.; Amendola, V.; Meneghetti, M. *Chem. Commun.* **2006**, 2394−2396. (c) Anémian, R.; Morel, Y.; Baldeck, P. L.; Paci, B.; Kretsch, K.; Nunzi, J.-M.; Andraud, C. *J. Mater. Chem.* **2003**, *13*, 2157−2163.
(3) (a) Kawata, S.; Sun, H.-B.; Tanaka, T.; Takada, K. *Nature* **2001**, *412*, 697−698. (b) Belfield, K. D.; Ren, X.; Van Stryland, E. W.; Hagan, D. J.; Dubikovsky, V.; Miesak, E. J. *J. Am. Chem. Soc.* **2000**, *122*, 1217−1218. (c) Klein, S.; Barsella, A.; Leblond, H.; Bulou, H.; Fort, A.; Andraud, C.; Lemercier, G.; Mulatier, J. C.; Dorkenoo, K. *Appl. Phys. Lett.* **2005**, *86*, 211118.
(4) For reviews, see: (a) Yuste, R. *Nature Methods* **2005**, *2*, 902−904. (b) Campagnola, P. J.; Loew, L. M. *Nat. Biotechnol.* **2003**, *21*, 1356−1360. (c) Zipfel, W. R.; Williams, R. M.; Webb, W. W. *Nat. Biotechnol.* **2003**, *21*, 1369−1377.
(5) (a) Nikolenko, V.; Yuste, R.; Zayat, L.; Baraldo, L. M.; Etchenique, R. *Chem. Commun.* **2005**, 1752−1754. (b) Wecksler, S. R.; Mikhailowsky, A.; Korystov, D.; Ford, P. C. *J. Am. Chem. Soc.* **2006**, *128*, 3831−3837.
(6) (a) Fredericksen, P. K.; Jorgensen, M.; Ogilby, P. R. *J. Am. Chem. Soc.* **2001**, *123*, 1215−1221. (b) Oar, M. A.; Serin, J. M.; Dichtel, W. R.; Fréchet, J. M. J.; Ohulchanskyy, T. Y.; Prasad, P. N. *Chem. Mater.* **2005**, *17*, 2267−2275.
(7) Porrès, L.; Mongin, O.; Katan, C.; Charlot, M.; Pons, T.; Mertz, J.; Blanchard-Desce, M. *Org. Lett.* **2004**, *6*, 47−50 and references therein.
(8) Dichtel, W. R.; Serin, J. M.; Edder, C.; Fréchet, J. M. J.; Matuszewski, M.; Tan, L.-S.; Ohulchanskyy, T. Y.; Prasad, P. N. *J. Am. Chem. Soc.* **2004**, *126*, 5380−5381.
(9) Zimmermann, J.; Linden, P. A.; Vaswani, H. M.; Hiller, R. G.; Fleming, G. R. *J. Phys. Chem. B* **2002**, *106*, 9418−9423.
(10) (a) Piszczek, G.; Maliwal, B. P.; Gryczynski, I.; Dattelbaum, J.; Lakowicz, J. R. *J. Fluoresc.* **2001**, *11*, 101−107. (b) White, G. F.; Litvinenko, K. L.; Meech, S. R. Andrew, D. L.; Thompson, A. J. *Photochem. Photobiol. Sci.* **2004**, *3*, 47−55.

10.1021/ic062181x CCC: $37.00
Published on Web 03/10/2007

Chart 1[a]

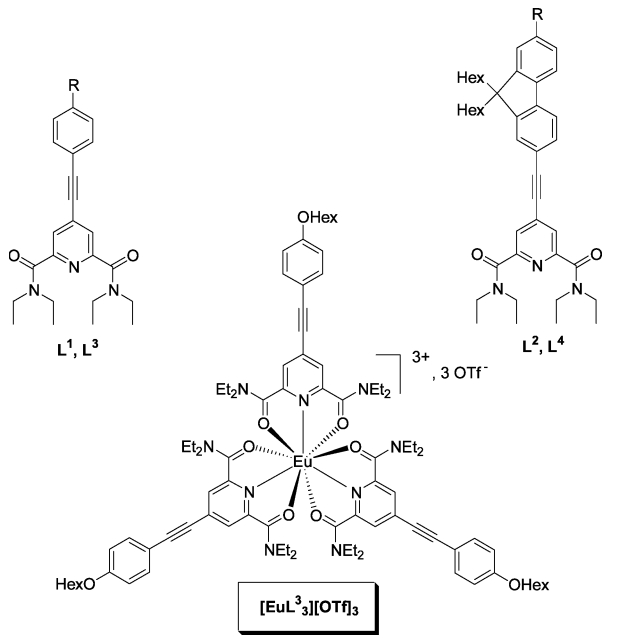

[a] $\mathbf{L^{1-2}}$, R = $NHex_2$; $\mathbf{L^{3-4}}$, R = OHex. For model $\mathbf{L^{3'}}$, R = OMe.

design of new chemical probes for bioimaging, combining the advantages of lanthanide luminescence (sharp emission, long lifetime, and insensitivity to oxygen) with those of two-photon excitation (confocal character and near-infrared excitation). Very recently, significant two-photon cross-sections were obtained to sensitize europium luminescence using dipolar ligands such as Michler's ketone (Mk)[11] or 2-(diethylanilin-4-yl)-4,6-bis(3,5-dimethylpyrazolyl)-triazine (dpbt).[12]

We previously reported that π-substituted dicarboxamide pyridine-based chromophores with dialkylamino donor groups ($\mathbf{L^{1-2}}$, Chart 1) feature excellent TPE fluorescence properties with high two-photon cross-sections.[13] Dicarboxamide pyridine ligands are well-known to complex lanthanide ions efficiently,[14] and the resulting 3:1 (L/M) complexes present the octupolar D_3 symmetry.[15] The great interest in this kind of symmetry has been widely shown for quadratic and cubic nonlinear optical effects[7,16] For both reasons, we decided to adapt these chromophores for the sensitization of europium(III) luminescence by the two photon antenna effect. Since chromophores $\mathbf{L^{1-2}}$ present charge transfer (CT) transitions at energies that are too low to allow the sensitization of Eu^{3+}, we decided to increase the level of the CT state by replacing the dialkylamino group by a weaker hexyloxy donor fragment ($\mathbf{L^{3-4}}$, Chart 1).

Experimental Section

Photophysical Measurements. UV−vis spectra in acetonitrile solution were recorded on Jasco V-550 or Biotek Instruments XS spectrophotometers. Quartz cuvettes with narrow (2 mm) path lengths were used to facilitate accurate measurement of the strong absorptions at the relatively high concentrations of complex (10^{-4} mol L^{-1}). The steady-state fluorescence spectra were measured using a Jobin Yvon Fluoromax-2 spectrofluorimeter, equipped with a red-sensitive Hamamatsu R928 photomultiplier tube. The emission spectra were corrected for the wavelength dependence of the PMT/emission monochromator by application of a correction curve generated from a standard lamp. Quantum yields of the ligands were obtained by standard serial dilution methods at high dilution (over the absorbance range of 0.005 − 0.05). In the case of the complexes, the slight tendency for some ligand dissociation to occur at high dilution rules out the use of concentrations that are significantly less than 10^{-4} mol L^{-1}. However, the influence of inner-filter effects in the measurement of the quantum yields, which can lead to under-estimated values because of excessive absorption, was minimized through the use of narrow path length (2 mm) cuvettes (excitation beam orientated through the narrow path) and by excitation into the low-energy tail of the absorbance band (abs < 0.05) rather than at its maximum. The 77 K emission spectra were obtained in an EPA glass, diethylether/isopentane/ethanol, 2:2:1, a solvent mixture with excellent glass-forming characteristics, using an Oxford Instruments DN1704 liquid-nitrogen-cooled cryostat. The fluorescence lifetimes of the ligands were measured by time-correlated single-photon counting, excited at 374.0 nm with an EPL-375 pulsed-diode laser at a repetition rate of 5 MHz (pulse length of ∼60 ps), and the emitted light was detected at 90° after passage through a monochromator using a Peltier-cooled R928. The lifetimes were extracted from the measured decays by reconvolution of the instrument response, which were obtained using a suspension of Ludox in water as a nonfluorescent scatterer. The luminescence lifetime of $[Eu\mathbf{L^3}_3][OTf]_3$ was measured by multichannel scaling, with data being collected over 2 ms at 1 μs/channel or over 4 ms at 2 μs/channel, following excitation with a xenon flashlamp operating at 100 Hz (pulse length of ∼2 μs). Light from the flashlamp was first passed through an excitation monochromator, and the measured lifetime was found to be independent of the excitation wavelength selected over the range investigated (360−410 nm).

Two-Photon Excited Luminescence Measurements. The TPA cross-section spectra were obtained by up-conversion fluorescence using a Ti:sapphire femtosecond laser in the range of 700−900 nm. The excitation beam is collimated over the cell length (10 mm). The fluorescence, collected at 90° to the excitation beam, was focused into an optical fiber connected to a spectrometer. The incident beam intensity was adjusted to ensure an intensity-squared dependence of the fluorescence over the whole spectral range. Calibration of the spectra was performed by comparison with the published 700−900 nm Coumarin-307 two-photon absorption spectrum.[17]

Computational Details. DFT geometry optimizations and TD-DFT excitation energy calculations on $\mathbf{L^{3'}}$, featuring a methoxy substituent, were carried out with the Gaussian 03 (revision B.04) package[18] employing the three-parameter hybrid functional of Becke

(11) Werts, M. H. V.; Nerambourg, N.; Pélégry, D.; Le Grand, Y.; Blanchard-Desce, M. *Photochem. Photobiol. Sci.* **2005**, *4*, 531−538.
(12) Fu, L.-M.; Wen, X.-F.; Ai, X.-C.; Sun, Y.; Wu, Y.-S.; Zhang, J.-P.; Wang, Y. *Angew. Chem., Int. Ed.* **2005**, *44*, 747−750.
(13) Barsu, C.; Fortrie, R.; Nowika, K.; Baldeck, P.; Vial, J.-C.; Fort, A.; Barsella, A.; Hissler M.; Bretonnière, Y.; Maury, O.; Andraud, C. *Chem. Commun*. **2006**, 4744−4746.
(14) Renaud, F.; Piguet, C.; Bernardinelli, G.; Bünzli, J.-C. G.; Hopfgartner, G. *Chem.—Eur. J.* **1997**, *3*, 1646−1659.
(15) For a review on octupolar theory, see : Ledoux, I.; Zyss, J. *Chem. Rev.* **1994**, *94*, 77−105.
(16) For selected examples of octupolar coordination complexes for quadratic nonlinear optics, see: (a) Maury, O.; Le Bozec, H. *Acc. Chem. Res.* **2005**, *38*, 691−704 and references therein. (b) Tancrez, N.; Feuvrie, C.; Ledoux, I.; Zyss, J.; Toupet, L.; Le Bozec, H.; Maury, O. *J. Am. Chem. Soc.* **2005**, *127*, 13474−13475.
(17) Xu, C.; Webb, W. W. *J. Opt. Soc. Am. B* **1996**, *13*, 481−491.

based on the correlation functional of Lee, Yang, and Parr (B3LYP).[19] The 6-31G* basis sets were used for all atoms.

General Considerations. The NMR spectra (^{1}H, ^{13}C, ^{19}F) were recorded at room temperature on a BRUKER AC 200 operating at 200.13 and 50.32 MHz for ^{1}H and ^{13}C, respectively, or on a VARIAN Unity Plus operating at 499.84 MHz for ^{1}H NMR. Data are listed in parts per million (ppm) and are reported relative to tetramethylsilane (^{1}H, ^{13}C), with residual solvent peaks being used as an internal standard (CHD_2CN ^{1}H, 1.93 ppm; ^{13}C (methyl), 1.3 ppm). Infrared spectra were recorded on a Mattson 3000 spectrometer using KBR pellets. High-resolution mass spectrometry measurements and elemental analysis were performed at the Service Central d'Analyze du CNRS (Vernaison, France).

4-(4-Hexyloxyphenyl)ethynyl)-2,6-bis(diethylcarbamoyl)pyridine (L^3). 4-Hexyloxyphenylacetylene (830 mg, 4.1 mmol, 1.1 equiv), copper iodide (140 mg, 0.74 mmol, 0.2 equiv), and $Pd(PPh_3)_2Cl_2$ (260 mg, 0.37 mmol, 0.1 equiv) were added to a degassed solution of 4-iodo-2,6-bis(diethylcarbamoyl)pyridine (1.5 g, 3.7 mmol, 1 equiv) in 20 mL of dry THF and 20 mL of dry Et_3N under argon. The brown mixture was heated to 40 °C in the dark, while stirring for 3 days. After the mixture was cooled to room temperature, the black precipitate was filtered and triturated with CH_2Cl_2 (2 × 20 mL). The remaining organic phase was washed with saturated ammonium chloride solution (3 × 50 mL) and brine (50 mL). The organic layer was then dried over anhydrous Na_2SO_4, and the solvent was evaporated under vacuum. The crude residue was purified by gradient flash chromatography over silica gel Si 60 (40−63 μm) (pentane/ethyl acetate from 9:1 to 1:1). The final product was obtained as a pale yellow solid (1.576 g, 89%). ^{1}H NMR (CD_3CN) : δ 7.59 (s, 2 H), 7.51 (d, $^3J_{HH}$ = 8.9 Hz, 2 H), 6.94 (d, $^3J_{HH}$ = 8.9 Hz, 2 H), 4.00 (t, $^3J_{HH}$ = 6.5 Hz, 2 H), 3.48 (q, $^3J_{HH}$ = 7.1 Hz, 4 H), 3.25 (q, $^3J_{HH}$ = 7.1 Hz, 4H), 1.74 (m, 2 H), 1.35 (m, 6 H), 1.18 (t, $^3J_{HH}$ = 7.1 Hz, 6 H), 1.08 (t, $^3J_{HH}$ = 7.1 Hz, 6 H), 0.89 (t, $^3J_{HH}$ = 7.1 Hz, 3 H). ^{13}C NMR (CD_3CN): δ 166.8, 159.9, 154.2, 133.13, 133.15, 123.2, 114.4, 112.7, 95.0, 84.4, 67.6, 42.4, 39.0, 30.8, 28.3, 24.8, 21.8, 13.1, 12.8, 11.6. UV: λ_{max} = 320 nm, ϵ = 28 600 L mol^{-1} cm^{-1}. IR (cm^{-1}): 2202 $\nu_{C\equiv C}$, 1624 $\nu_{C=O}$. Elemental Analysis Calcd (%) for $C_{29}H_{39}N_3O_3$: C, 72.92; H, 8.23; N, 8.80. Found: C, 72.93; H, 8.29; N, 8.27. Mass Calcd: 500.2889. Found: 500.2894 $[M + Na]^+$.

4-(2-(7-Hexyloxy-9,9′-dihexylfluorenyl)ethynyl)-2,6-bis(diethylcarbamoyl)pyridine (L^4). 2-(7-Hexyloxy-9,9′-dihexylfluorenyl)-acetylene (308 mg, 0.672 mmol, 1 equiv), copper iodide (25.5 mg, 0.134 mmol, 0.2 equiv), and $Pd(PPh_3)_2Cl_2$ (47.2 mg, 0.0672 mmol, 0.1 equiv) were added to a degassed solution of 4-iodo-2,6-bis-(diethylcarbamoyl)pyridine (0.271 g, 0.672 mmol, 1 equiv) in 20 mL of dry THF and 10 mL of dry Et_3N under argon. The brown mixture was heated to 50 °C in the dark and was stirred for 24 h. After the mixture was cooled to room temperature, the black precipitate was filtered and triturated with pentane (2 × 20 mL). The remaining organic phase was washed with saturated ammonium chloride solution (3 × 50 mL) and brine (50 mL). The organic layer was then dried over Na_2SO_4 and evaporated under vacuum. The crude residue was purified by flash chromatography over silica gel Si 60 (40−63 μm) (pentane/ethyl acetate 2/1). The final product was obtained as a pale yellow solid (0.32 g, 65%). ^{1}H NMR (CD_3CN): δ 7.67 (s, 2 H), 7.56 (m, 2H), 7.44 (m, 2H), 6.85 (m, 2H), 4.00 (t, $^3J_{HH}$ = 6.6 Hz, 2H), 3.54 (q, $^3J_{HH}$ = 7.1 Hz, 4H), 3.32 (q, $^3J_{HH}$ = 7.1 Hz, 4H), 1.88 (m, 6H), 1.44 (m, 2H), 1.34 (m, 4H), 1.24 (t, $^3J_{HH}$ = 7.1 Hz, 6H), 1.14 (t, $^3J_{HH}$ = 7.1 Hz, 6H), 1.03 (m, 12H), 0.90 (t, $^3J_{HH}$ = 6.8 Hz, 3H), 0.74 (t, $^3J_{HH}$ = 6.1 Hz, 6H), 0.59 (m, 4H). ^{13}C NMR (CD_3CN): δ 167.69, 159.83, 153.81, 153.31, 150.45, 142.85, 134.11, 133.0, 131.19; 126.22, 125.23, 121.05, 118.88, 118.46, 113.19, 109.41, 97.35, 85.95, 68.38, 55.18, 43.29, 40.48, 40.20, 31.68, 31.52, 29.70, 29.35, 25.79, 23.68, 22.612, 22.61, 14.30, 14.05, 14.00, 12.80. UV: λ_{max} = 349 nm, ϵ = 43 000 L mol^{-1} cm^{-1}. IR (cm^{-1}): 2212 $\nu_{C\equiv C}$, 1633 $\nu_{C=O}$. mp: 130 °C. Elemental Anal. Calcd (%) for $C_{48}H_{67}N_3O_3$: C, 78.54; H, 9.20; N, 5.72. Found: C, 78.49; H, 9.25; N, 5.54.

[EuL^3_3][OTf]$_3$. $Eu(OTf)_3$ (125.5 mg, 0.21 mmol, 1 equiv) was added to a solution of L^3 (300 mg, 0.63 mmol, 3 equiv) in 20 mL of dry THF under argon. The bright yellow mixture was stirred at room temperature for 2 h. The solvent was then evaporated under vacuum, and the crude residue was washed with pentane (2 × 10 mL) and diethyl ether (2 × 10 mL). The complex was obtained as a bright yellow solid (332 mg, 78%). ^{1}H NMR (CD_3CN): δ 7.34 (d, $^3J_{HH}$ = 8.7 Hz, 6 H), 6.90 (d, $^3J_{HH}$ = 8.7 Hz, 6 H), 6.16 (s, 6 H), 3.96 (t, $^3J_{HH}$ = 6.5 Hz, 6 H), 3.68 (m, 24 H), 1.70 (m, 6 H), 1.43 (m 18 H), 1.25 (m, 36 H), 0.86 (t, $^3J_{HH}$ = 6.3 Hz, 9 H). ^{13}C NMR (CD_3CN): δ 164.0, 162.4, 148.6, 146.0, 135.5, 116.0, 112.3, 103.0, 97.2, 81.2, 69.3, 43.0, 42.9, 32.3, 29.8, 26.3, 23.3, 15.6, 14.4, 13.6. ^{19}F NMR (CD_3CN): δ −79.6. UV: λ_{max} = 360 nm, ϵ = 75 000 L mol^{-1} cm^{-1}. IR (cm^{-1}): 2206 $\nu_{C\equiv C}$, 1603 $\nu_{C=O}$. Elemental Anal. Calcd (%) for $C_{90}H_{117}EuF_9N_9O_{18}S_3{\cdot}3H_2O$: C, 51.82; H, 5.94; N, 6.04. Found: C, 51.72; H, 5.78; N, 6.24.

[EuL^4_3][OTf]$_3$. $Eu(OTf)_3$ (54.4 mg, 0.0908 mmol, 1 equiv) was added to a solution of L^4 (200 mg, 0.272 mmol, 3 eq) in 10 mL of dry THF under argon. The bright yellow mixture was stirred at room temperature for 2 h. The solvent was then evaporated under vacuum, and the crude residue was dissolved in a minimum of CH_2Cl_2. The solution was then precipitated and triturated with pentane (2 × 10 mL). The complex was obtained as a bright yellow solid (210 mg, 82%). ^{1}H NMR (CD_3CN): δ 7.6 (m, 6 H), 7.3 (m, 6 H), 6.9 (m, 6 H), 6.2 (b, 6 H), 4.00 (t, $^3J_{HH}$ = 6.4 Hz, 6 H), 3.7 (b, 12 H), 2.9 (b, 12 H), 1.9−1.6 (m, 18 H), 1.6−1.2 (m, 42 H), 1.2−0.8 (m, 45 H), 0.71 (t, $^3J_{HH}$ = 6.1 Hz, 18 H), 0.5−0.3 (m, 24 H). ^{13}C NMR (CD_3CN): δ 160.4, 153.4, 150.4, 147.4, 144.2, 139.4, 132.3, 132.1, 126.8, 121.5, 118.9, 117.2, 116.3, 113.9, 109.1, 102.6, 96.0, 80.6, 68.2, 55.2, 41.4, 39.7, 31.3, 31.2, 29.1, 28.9, 25.4, 23.5, 22.3, 22.2, 14.3, 13.3, 13.2, 12.1. ^{19}F NMR (CD_3CN): δ −78.5. UV: λ_{max} = 399 nm, ϵ = 85 000 L mol^{-1} cm^{-1}. IR (cm^{-1}): 2204 $\nu_{C\equiv C}$, 1604 $\nu_{C=O}$. Elemental Anal. Calcd (%) for $C_{147}H_{201}EuF_9N_9O_{18}S_3{\cdot}3CH_2Cl_2$: C, 58.95; H, 6.83; N, 4.12. Found: C, 58.32; H, 6.77; N, 4.13.

Results and Discussion

Synthesis of Ligands and Complexes. Ligands L^3 and L^4 were prepared by Sonogashira cross-coupling between

(18) Frisch, M. J.; Trucks, G. W.; Schlegel, H. B.; Scuseria, G. E.; Robb, M. A.; Cheeseman, J. R.; Montgomery, J. A., Jr.; Vreven, T.; Kudin, K. N.; Burant, J. C.; Millam, J. M.; Iyengar, S. S.; Tomasi, J.; Barone, V.; Mennucci, B.; Cossi, M.; Scalmani, G.; Rega, N.; Petersson, G. A.; Nakatsuji, H.; Hada, M.; Ehara, M.; Toyota, K.; Fukuda, R.; Hasegawa, J.; Ishida, M.; Nakajima, T.; Honda, Y.; Kitao, O.; Nakai, H.; Klene, M.; Li, X.; Knox, J. E.; Hratchian, H. P.; Cross, J. B.; Bakken, V.; Adamo, C.; Jaramillo, J.; Gomperts, R.; Stratmann, R. E.; Yazyev, O.; Austin, A. J.; Cammi, R.; Pomelli, C.; Ochterski, J. W.; Ayala, P. Y.; Morokuma, K.; Voth, G. A.; Salvador, P.; Dannenberg, J. J.; Zakrzewski, V. G.; Dapprich, S.; Daniels, A. D.; Strain, M. C.; Farkas, O.; Malick, D. K.; Rabuck, A. D.; Raghavachari, K.; Foresman, J. B.; Ortiz, J. V.; Cui, Q.; Baboul, A. G.; Clifford, S.; Cioslowski, J.; Stefanov, B. B.; Liu, G.; Liashenko, A.; Piskorz, P.; Komaromi, I.; Martin, R. L.; Fox, D. J.; Keith, T.; Al-Laham, M. A.; Peng, C. Y.; Nanayakkara, A.; Challacombe, M.; Gill, P. M. W.; Johnson, B.; Chen, W.; Wong, M. W.; Gonzalez, C.; Pople, J. A. *Gaussian 03*, revision B.04; Gaussian, Inc.: Wallingford, CT, 2004.
(19) (a) Lee, C. T.; Yang, W. T.; Parr, R. G. *Phys. Rev. B* **1988**, *37*, 785−789. (b) Becke, A. D. *J. Chem. Phys.* **1993**, *98*, 5648−5652.

Scheme 1. Synthesis of $\mathbf{L^3}$ and $\mathbf{L^4}$

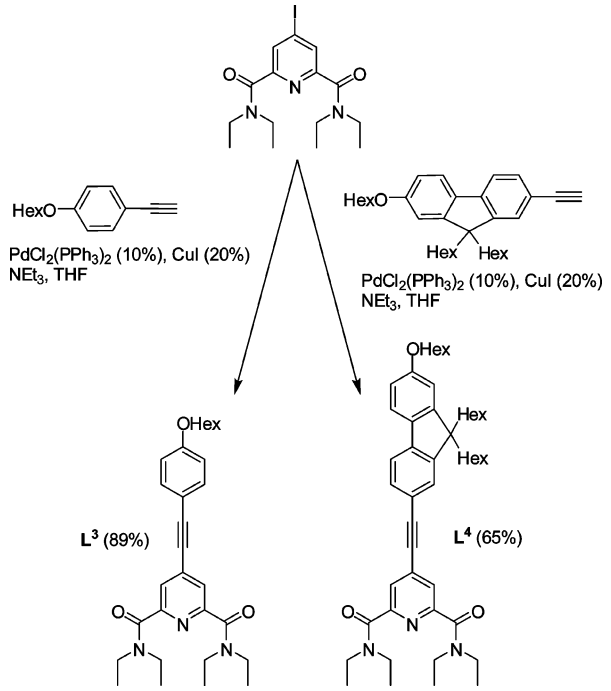

4-iodo-2,6-bis(diethylcarbamoyl)pyridine[13] and the corresponding hexyloxy-aryl-acetylene (aryl = phenyl or fluorenyl), in yields of 89 and 65%, respectively, after chromatographic purification (Scheme 1). The coordination of three equivalents of $\mathbf{L^{3-4}}$ to europium triflate was carried out in THF at room temperature for 2 h. After evaporation of the solvents, the residue was dissolved in the minimum amount of CH_2Cl_2 and triturated with pentane. Upon filtration, the complexes $[Eu\mathbf{L^3}_3][OTf]_3$ and $[Eu\mathbf{L^4}_3][OTf]_3$ were obtained as yellow powders in 78 and 82% yields, respectively. All the compounds were fully characterized by NMR and IR spectroscopies and by elemental analysis. The elemental analysis confirms the 3:1 ratio between ligands and metal, while the ^1H and ^{13}C NMR spectra of the complexes (CD_3CN, RT (room temp)) exhibit only one set of signals in agreement with the D_3 symmetrical architecture. Complexation to the paramagnetic europium(III) center results in a downfield shift of the pyridinic protons from 7.59 ($\mathbf{L^3}$) to 6.16 pm. In addition, the IR spectrum of the complex shows two bands at 2206 and 1603 cm^{-1} characteristic of $\nu_{C\equiv C}$ and $\nu_{C=O}$ vibrations, the latter being shifted to lower energy upon complexation ($\Delta\nu_{C=O} = 21\ cm^{-1}$).[14]

Photophysical Properties. Linear Absorption and Emission. All photophysical properties were studied in acetonitrile at 10^{-5} mol L^{-1} for the ligands and 10^{-4} mol L^{-1} for the complexes because of the partial dissociation at lower concentration. $\mathbf{L^3}$ presents a broad absorption band centered at 320 nm with a shoulder around 300 nm and a second band at higher energy (250 nm) (Figure 1 and Table 1). TD-DFT calculations performed on model $\mathbf{L^{3'}}$, featuring a methoxy substituent, clearly indicate that the lowest-energy transition ($\lambda^{TH} = 333$ nm) presents marked CT character, with the HOMO and the LUMO being mainly located at the alkoxy donor and pyridine acceptor parts of the molecule, respectively (Figure 2). The shoulder can be tentatively assigned

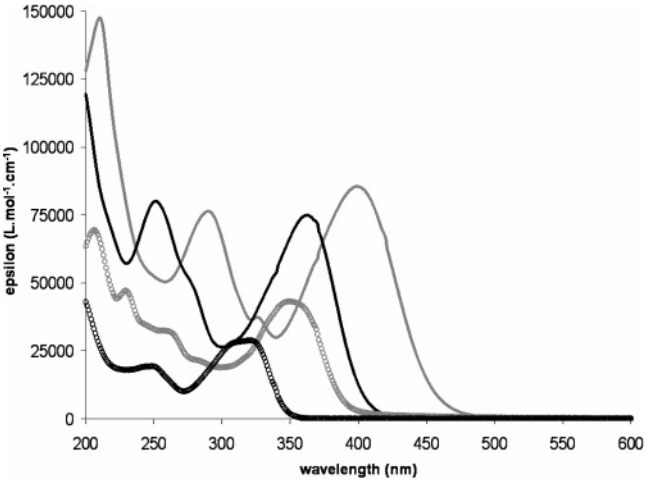

Figure 1. Absorption spectra of $\mathbf{L^3}$ (gray ○), $\mathbf{L^4}$ (black ○), $[Eu\mathbf{L^3}_3][OTf]_3$ (gray —), and $[Eu\mathbf{L^4}_3][OTf]_3$ (black —) in acetonitrile solution (RT).

Table 1. Linear and Nonlinear Optical Data Measured at Room Temperature in Acetonitrile Solution

	$\mathbf{L^3}$	$\mathbf{L^4}$	$[Eu\mathbf{L^3}_3][OTf]_3$	$[Eu\mathbf{L^4}_3][OTf]_3$
λ_{max}[a] (nm)	320	349	360[b]	399[b]
ϵ (L mol^{-1} cm^{-1})	29 000	43 000	75 000	85 000
λ_{em} (nm)	427	473	595, 617, 690, 697	
Φ_{lum}	0.03[c]	0.89[c]	0.056[b,d]	
τ	2.9 (1.0[e]) ns	2.1 ns	270 μs	

[a] λ_{max} for the lowest-energy absorption maximum. [b] $c = 10^{-4}$ mol L^{-1}. [c] Measured using quinine sulfate in 1 M H_2SO_4 as the standard. [d] Measured using $[Ru(bpy)_3]Cl_2$ in H_2O as the standard. [e] Minor component to observed biexponential decay.

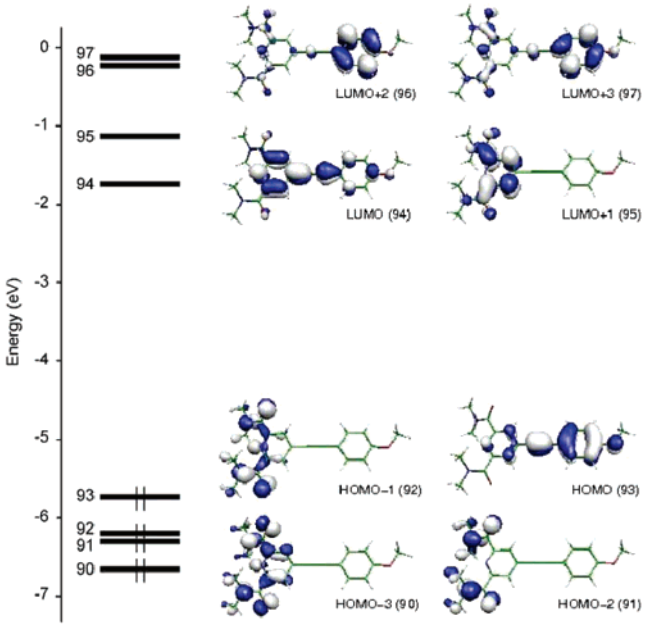

Figure 2. Molecular orbital energy diagram for $\mathbf{L^{3'}}$ (B3LYP/6-31G*).

to an overlap of less intense $\pi-\pi^*$ and $n-\pi^*$ transitions from the amide side arms to the central pyridinic ring,[14] while the higher-energy transition (250 nm) presents a major contribution from the HOMO → LUMO+3 monoelectronic transition localized in the π-conjugated system and generally designated as a locally excited (LE) transition (Table 2). This ligand is moderately fluorescent, displaying a broad struc-

Table 2. TD-DFT Calculated Singlet−Singlet Excitation Energies (E), Corresponding Wavelengths (λ), and Oscillator Strengths (f) for $\mathbf{L}^{3'}$ (B3LYP/6-31G*)[a]

E (eV)	λ (nm)	f	composition (C)
3.727	333	0.992	93 → 94 (0.65)
			85 → 99 (−0.10)
3.895	318	0.012	92 → 94 (0.58)
			90 → 94 (0.26)
			93 → 95 (0.21)
4.058	306	0.019	91 → 94 (0.67)
			89 → 94 (−0.15)
4.191	296	0.012	90 → 94 (0.54)
			93 → 95 (−0.32)
			92 → 94 (−0.19)
			87 → 94 (−0.19)
4.706	263	0.055	87 → 94 (0.40)
			91 → 95 (−0.38)
			89 → 95 (−0.31)
			84 → 94 (0.21)
			93 → 95 (−0.11)
4.766	260	0.061	90 → 95 (0.57)
			92 → 95 (−0.36)
4.782	259	0.024	87 → 94 (0.38)
			91 → 95 (0.35)
			89 → 95 (0.32)
			84 → 94 (0.16)
			90 → 94 (0.13)
			86 → 95 (0.12)
5.001	247	0.246	93 → 97 (0.47)
			86 → 94 (0.41)
			93 → 96 (0.27)
			85 → 99 (−0.11)
			88 → 94 (−0.10)
5.175	240	0.050	88 → 94 (0.40)
			93 → 96 (0.34)
			87 → 95 (0.31)
			84 → 95 (0.22)
			88 → 97 (−0.12)

[a] Only the transitions with a calculated oscillator strength higher than 0.010 are reported.

tureless emission band centered at 427 nm with a quantum yield of 0.03 at RT, arising from the CT state.

At 77 K, the fluorescence band is sharper, structured, and strongly blue shifted to $\lambda_{max} = 364$ nm, suggesting that, under these conditions, the emission may originate from the ^{1}LE instead of the CT state. This trend is similar to that observed in the case of other charge-transfer chromophores, such as PODAN.[20] Excited states with CT character are generally destabilized substantially more than $\pi-\pi^*$ transitions in frozen glasses because of the higher degree of solvent reorganization that accompanies formation of the CT states at RT, which is inhibited in the glass. In addition, a weak structured phosphorescence is observed from which the triplet state (^{3}LE) energy is estimated to be 21 300 cm^{-1} (Figure 3). In the case of $\mathbf{L^4}$, featuring an extended π-conjugated fluorenyl −C≡C− backbone, both the lowest-energy absorption band and the emission are shifted toward lower energies (λ_{max} = 349 nm, λ_{em}(CT) = 473 nm). This compound is intensely fluorescent in solution: replacement of the phenyl by the fluorenyl moiety induces a dramatic enhancement of the quantum yield efficiency from 0.03 for $\mathbf{L^3}$ up to 0.89 for $\mathbf{L^4}$. Again, the fluorescence is strongly

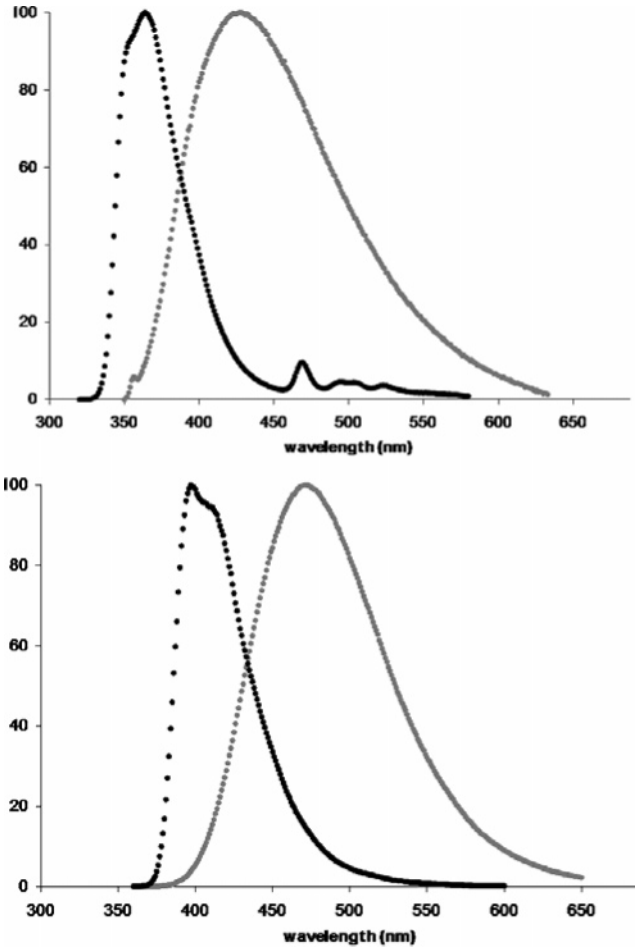

Figure 3. Luminescence of $\mathbf{L^3}$ (top, λ_{ex} = 330 nm) and $\mathbf{L^4}$ (bottom, λ_{ex} = 350 nm) in acetonitrile solution at room temperature (gray ●) and in an EPA glass at 77 K (black ●).

blue shifted upon cooling to 77 K ($\lambda_{em}(^1\text{LE}) = 390$ nm), but in this case, no phosphorescence is detected (Figure 3).

For both ligands, complexation to europium results in a large bathochromic shift of the CT transition in the UV−vis spectra ($\Delta\lambda$ = 40−50 nm, Table 1) because the strong Lewis acidity of the metal ion enhances the acceptor strength of the pyridine moieties.[21] Upon excitation into the ligand CT band of [Eu$\mathbf{L^3}_3$][OTf]$_3$, the characteristic bright-red long-lived luminescence of europium(III) is observed. The emission spectrum (Figure 4) exhibits the five bands expected for the $^5D_0 \rightarrow {}^7F_J$ (J = 0−4) transitions, with a very intense $^5D_0 \rightarrow {}^7F_2$ transition, and the excitation spectrum registered at each of the emission bands shows a good match to the absorption spectrum (an example is provided in Figure 5). The temporal decay of the emission following pulsed excitation follows monoexponential kinetics, confirming the presence of a single dominant species in solution under these conditions (Figure 5). The measured lifetime of 270 μs was not significantly different in deuterated solvent (CD_3CN), ruling out the process of energy transfer into solvent C−H vibrations as a decay pathway for the Eu(III) $^5D_0$ excited state. The quantum yield is rather modest (0.056), although

(20) It is well known that the formation of CT excited states is normally a thermally assisted process, see: *Principles of Fluorescence Spectroscopy*, 2nd ed.; Lakowicz, J. R., Ed.; Kluwer: New York, 1999; Chapter 6, pp 200−201 and references therein.

(21) Sénéchal-David, K.; Hemeryck, A.; Tancrez, N.; Toupet, L.; Williams, J. A. G.; Ledoux, I.; Zyss, J.; Boucekkine, A.; Guégan, J.-P.; Le Bozec, H.; Maury, O. *J. Am. Chem. Soc.* **2006**, *128*, 12243−12255.

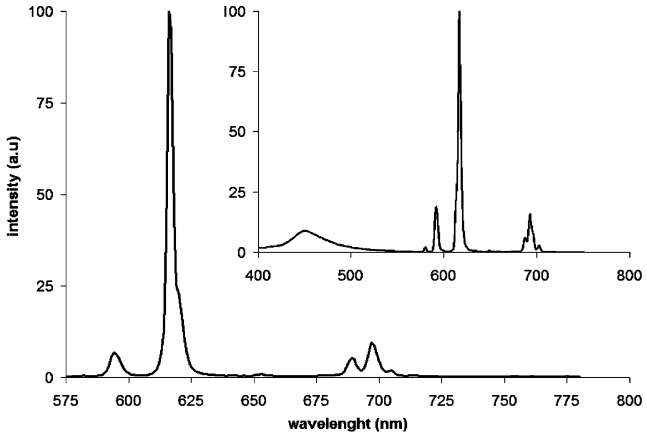

Figure 4. Emission spectra of [Eu$\mathbf{L}^3_3$][OTf]$_3$ at RT in acetonitrile solution (λ_{ex} = 400 nm) and [Eu$\mathbf{L}^4_3$][OTf]$_3$ at 77 K in an EPA glass (inset, λ_{ex} = 430 nm).

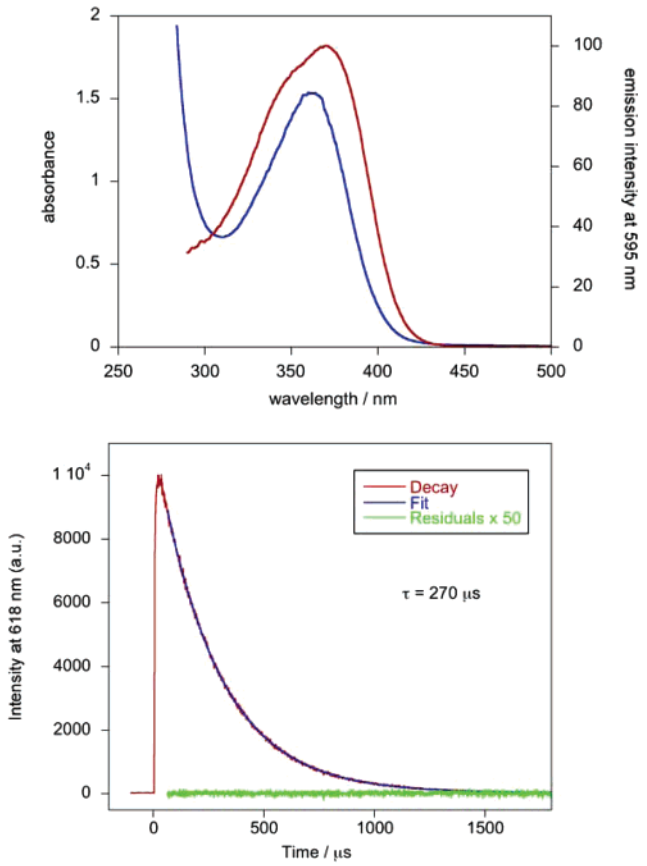

Figure 5. (top) Absorption spectrum (blue) and excitation spectrum (red; λ_{em} = 595 nm) of [Eu$\mathbf{L}^3_3$][OTf]$_3$ in acetonitrile (10^{-4} mol L^{-1}) measured in a 2 mm path length cuvette at 298 K. (bottom) Representative emission decay in acetonitrile (10^{-4} mol L^{-1}) at 298 K (red line). The best-fit to a single-exponential decay is shown in blue. The decay is monoexponential, confirming that only one species is present in significant amounts under these conditions.

this should be regarded as a lower limit, as explained in the Experimental Section. Moreover, since the absorption is high and the bulk of the emission is concentrated in the hypersensitive ΔJ = 2 band, the emitted red light within this narrow wavelength region is intense. Energy transfer from the ligand to the metal in this complex is likely to be facilitated by a favorable overlap integral between the ligand

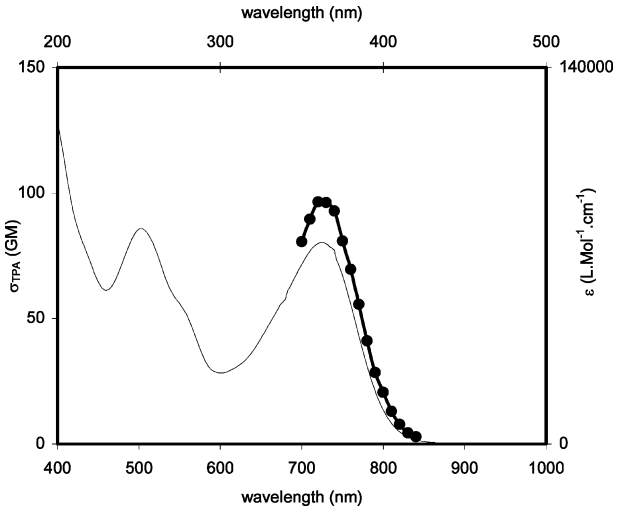

Figure 6. Two-photon excitation spectrum of [Eu$\mathbf{L}^3_3$][OTf]$_3$ in acetonitrile solution (●, lower abscissa). Superimposed on this plot is the single-photon absorption spectrum (—, upper abscissa).

donor state and the acceptor states on the europium(III) ion that are $^5D_2$ (21 300 cm^{-1}), $^5D_1$ (19 000 cm^{-1}), and emissive $^5D_0$ (17 400 cm^{-1}) states. It is generally acknowledged that sensitization of Eu^{3+} luminescence proceeds via the triplet state of the chromophore, although direct sensitization from the singlet CT state has also been envisioned.[22]

In contrast, in the case of [Eu$\mathbf{L}^4_3$][OTf]$_3$, no significant emission is observed at room temperature, but interestingly, the characteristic Eu^{3+} emission profile reappears upon cooling to 77 K (Figure 4, inset). It is likely that either the CT or the triplet state of $\mathbf{L}^4$ at room temperature lies too low in energy to sensitize the europium ion. Indeed, even if the donor state of this ligand is still slightly higher than the Eu^{3+} $^5D_0$ state, too small gap will lead to rapid, thermally activated back-energy transfer at room temperature, thus quenching the emission.

The observation of metal-based emission at 77 K can then be tentatively rationalized according to the strong influence of temperature on the energy of charge-transfer excited states.[20] In a frozen glass at low temperature, the charge-transfer process is disfavored, leading to a shift in the CT state to higher energy. Energy transfer to Eu^{3+} $^5D_0$ may then occur either directly from the CT state, or the CT state may even be raised to an energy higher than that of the locally excited state, allowing the latter to be populated, from which energy transfer occurs. We are not able to distinguish between the two possibilities, which ultimately differ only in the extent of charge-transfer in the donor state.

Two-Photon Absorption Processes. The two-photon absorption cross-section (σ_{TPA}) was measured by the two-photon excited luminescence technique using a femtosecond Ti:sapphire laser as the excitation source and coumarin-307 as a standard. Because the measurements were done in acetonitrile at room temperature, only the complex [Eu$\mathbf{L}^3_3$]-[OTf]$_3$ was considered, and the europium(III) luminescence

(22) Yang, C.; Fu, L.-M.; Wang, Y.; Zhang, J.-P.; Wong, W.-T.; Ai, X.-C.; Qiao, Y.-F.; Zou, B.-S.; Gui, L.-L. *Angew. Chem., Int. Ed.* **2004**, *43*, 5010−5013.

spectrum was observed upon irradiation between 700 and 900 nm. Figure 6 reports the calibrated two-photon excitation spectrum, and for comparison, the single-photon absorption spectrum has been superimposed using the wavelength-doubled scale in the upper abscissa. As expected for noncentrosymmetric chromophores, because of the absorption selection rules, a strong correlation is observed between the two spectra, indicating that the excited states involved in the one- or two-photon processes are the same. The maximum two-photon absorption cross-section, estimated to be 96 GM at 720 nm is slightly lower, although in the same range as that of the best dipolar lanthanide complexes ($MkEu(fod)_3$, 253 GM at 810 nm[11] and $dtpaEu(tta)_3$, 157 GM at 810 nm[12]). However, it should be noted that this performance is achieved at a significantly shorter wavelength. For a similar activity, the maximal two-photon absorption wavelength is significantly blue shifted in the case of the octupolar $[Eu\mathbf{L}^{3}_{3}][OTf]_3$, compared to the previously cited complexes ($\Delta\lambda = 90$ nm). This result is in agreement with the better transparency/nonlinearity tradeoff observed in the case of octupolar derivatives.[23]

Summary

In conclusion, in this article, we described the synthesis and photophysical properties of two new dicarboxamide pyridine-based chromophores designed for the sensitization of europium(III) luminescence by the two-photon antenna effect. The particular influence of the octupolar symmetry has been underlined and further studies are currently being conducted to adapt this complex to biological media for nonlinear microscopy imaging purposes.

Acknowledgment. The authors thank the Agence Nationale pour la Recherche, France (ANR LnOnL NT05-3_42676) and EPSRC, U.K., for financial support and H. Le Bozec for fruitful discussions.

IC062181X

(23) (a) Katan, C.; Terenziani, F.; Mongin, O.; Werts, M. H. V.; Porrès, L.; Pons, T.; Mertz, J.; Tretiak, S.; Blanchard-Desce, M. *J. Phys. Chem. A* **2005**, *109*, 3024−3037. (b) Maury, O.; Viau, L.; Sénéchal, K.; Corre, B.; Guégan, J.-P.; Renouard, T.; Ledoux, I.; Zyss, J.; Le Bozec, H. *Chem.—Eur. J.* **2004**, *10*, 4454−4466. (c) Sénéchal, K.; Maury, O.; Le Bozec, H.; Ledoux, I.; Zyss, J. *J. Am. Chem. Soc.* **2002**, *124*, 4561−4562.